Correspondence

Beyond Intelligent Reflecting Surfaces: Reflective-Transmissive Metasurface Aided Communications for Full-Dimensional Coverage Extension

Shuhang Zhang, *Student Member, IEEE*, Hongliang Zhang, *Member, IEEE*, Boya Di, *Member, IEEE*, Yunhua Tan, Zhu Han, *Fellow, IEEE*, and Lingyang Song, *Fellow, IEEE*

***Abstract*—In this paper, we study an intelligent omni-surface (IOS)-assisted downlink communication system, where the link quality of a mobile user (MU) can be improved with a proper IOS phase shift design. Unlike the intelligent reflecting surface (IRS) in most existing works that only forwards the signals in a reflective way, the IOS is capable to forward the received signals to the MU in either a reflective or a transmissive manner, thereby enhancing the wireless coverage. We formulate an IOS phase shift optimization problem to maximize the downlink spectral efficiency (SE) of the MU. The optimal phase shift of the IOS is analysed, and a branch-and-bound based algorithm is proposed to design the IOS phase shift in a finite set. Simulation results show that the IOS-assisted system can extend the coverage significantly when compared to the IRS-assisted system with only reflective signals.**

***Index Terms*—Intelligent omni-surface, IOS phase shift design, coverage extension.**

I. Introduction

With the development of meta-surfaces, the intelligent reflecting surface (IRS) is considered as a promising technique for future communications, since it is cost-effective to achieve a high spectral and energy efficiency [1]. The IRS contains a large number of elements with controllable electromagnetic responses that can shape the propagation environment into a desirable form [2], thus enhancing the quality of the communication links [3]. In the literature, some initial works have studied the utilization of wave-reflective IRS to assist the wireless communication networks. In [4], a joint power allocation and continuous phase shift design has been studied in a reflective IRS-assisted system to maximize energy efficiency. In [5], the achievable data rate of a reflective IRS-assisted communication system has been evaluated, and the effect of limited phase shifts on the data rate has been investigated. However, in the existed works, the signal arrived at the IRS is considered to be reflected completely. As a result, the receivers on the other side of the IRS are shielded, which leads to an incomplete wireless coverage.

In this paper, we study an intelligent omni-surface (IOS), whose received signals can be transmitted and reflected to both sides concurrently. We utilize the IOS in a communication system to extend the service coverage for downlink transmissions. The IOS provides an ubiquitous wireless coverage for the mobile user (MU) on its either side, and the propagation environment of the MU can be adjusted via the phase shifts of the electrically controllable elements on the IOS.

The implementation of the IOS-assisted communication system has also brought some new challenges. *First*, the power of reflective and transmissive signals of the IOS may not be symmetric, i.e., the channel model of the reflective signal and the transmissive signal can be different. Therefore, the studies on the reflective IRS-assisted communications cannot be applied directly in the IOS-assisted ones. *Second*, the direct communication link from the base station (BS) to the MU may exist concurrently with the reflective and transmissive links in the IOS-assisted communication system. Such a superposition impact of multiple communication links should be considered for IOS phase shift design.

To deal with the above challenges, we first propose a novel model for the IOS with a controllable electromagnetic response on both sides, and then introduce its physical characteristics. Based on the channel model of the proposed IOS, we formulate a downlink communication spectral efficiency (SE) maximization problem, where an IOS is utilized to improve the SE of a MU by proper phase shift design. The optimal solution to the IOS phase shift is analysed, and a branch-and-bound algorithm is proposed to design the IOS phase shifts in a finite set. The performances in terms of coverage and SE improvement are provided by simulations.

The rest of this paper is organized as follows. In Section II, we introduce the IOS. In Section III, we present an IOS-assisted downlink communication system, including the channel model and the SE, and formulate a SE maximization problem with IOS phase shift design. An IOS phase shift design algorithm is provided in Section IV. Numerical results in Section V evaluate the performance of the proposed algorithm. Finally, we draw the conclusions in Section VI.

II. Intelligent Omni-Surface

The IOS is a two-dimensional array of electrically controllable IOS elements. Each element in the IOS is of the same size, with δ_x being the width and δ_y being the height, and is composed of multiple metal patches and N_D PIN diodes assembled on dielectric substrates. As shown in Fig. 1, the metal patches are connected to the ground via PIN diodes, and can be switched between *ON* and *OFF* states according to the applied bias voltages, based on which a unique phase shift can be added to the transmissive and reflective signals. There are 2^{N_D} possible phase shifts in total for each element. For generality, we assume that a subset of possible phase shifts are available, which is referred to as the

Manuscript received June 3, 2020; revised August 30, 2020; accepted September 12, 2020. Date of publication September 18, 2020; date of current version November 12, 2020. This work was supported in part by the National Natural Science Foundation of China under Grants 61625101, 61829101, and 61941101 and in part by NSF under Grants EARS-1839818, CNS-1717454, CNS-1731424, and CNS-1702850. The review of this article was coordinated by Prof. Yong Liang Guan. *(Corresponding author: Lingyang Song.)*

Shuhang Zhang, Yunhua Tan, and Lingyang Song are with the Department of Electronics, Peking University, Beijing 100871, China (e-mail: shuhangzhang@pku.edu.cn; tanggeric@pku.edu.cn; lingyang.song@pku.edu.cn).

Hongliang Zhang is with the Department of Electronics, Peking University, Beijing 100871, China, and also with the Department of Electrical Engineering, Princeton University, Princeton, NJ 08544 USA (e-mail: hongliang.zhang92@gmail.com).

Boya Di is with the Department of Electronics, Peking University, Beijing 100871, China, and also with the Department of Computing, Imperial College London, London SW7 2BU, U.K. (e-mail: diboya92@gmail.com).

Zhu Han is with the Electrical and Computer Engineering Department, University of Houston, Houston, TX 77004 USA, and also with the Department of Computer Science and Engineering, Kyung Hee University, Seoul 02447, South Korea (e-mail: zhan2@uh.edu).

Digital Object Identifier 10.1109/TVT.2020.3024756

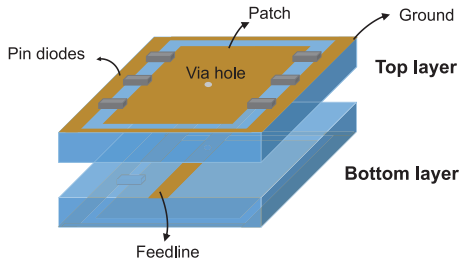

Fig. 1. Schematic structure of an IOS element.

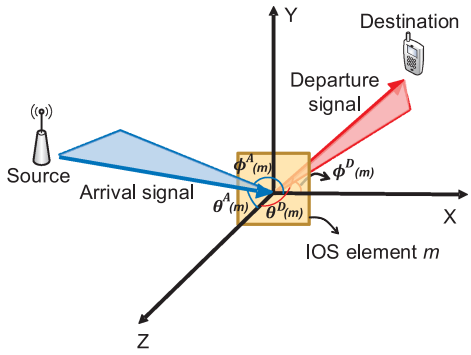

Fig. 2. Illustration for the angles of arrival and departure signals for a IOS element.

available phase shifts set, denoted by $\mathcal{S}_a = \{1, \ldots, S_a\}$. We denote the phase shifts of the mth element by $s_m \in \mathcal{S}_a$. We can control the PIN diodes to generate S_a patterns of phase shifts for each element, with a uniform interval $\Delta\psi_m = \frac{2\pi}{S_a}$ [5]. The possible phase shift value can be given as $l_m \Delta\psi_m$, where l_m is an integer satisfying $0 \leq l_m \leq S_a - 1$. The phase shift of the IOS is defined as the vector of the phase shifts of all IOS elements, i.e., $\boldsymbol{s} = (s_1, \ldots, s_M)$, where M denotes the number of IOS elements. When a signal arrives at an IOS element from either side of it, a part of the signal transmits through the elements as the *transmissive signal*, and the other part of the signal is reflected as the *reflective signal* [6]. The phase shift of the IOS determines the waveform of the transmissive and reflective signals concurrently.

As illustrated in Fig. 2, we denote the direction of the arrival signal from the source node to element m, and the direction from element m to the destination node by $\xi^A(m) = (\theta^A(m), \phi^A(m))$ and $\xi^D(m) = (\theta^D(m), \phi^D(m))$, respectively. The influence of element m on the arrival signal is denoted by a complex number g_m, which we refer to as the *power gain* of the signal. The value of g_m for a transmission link is affected by the direction of the arrival signal from the source node, i.e., $\xi^A(m)$, the direction of the departure signal to the destination node, i.e., $\xi^D(m)$, and the element phase shifts s_m. The experimental equation of the corresponding power gain can be expressed as [7]

$$g_m(\xi^A(m), \xi^D(m), s_m) = \sqrt{G_m K^A(m) K^D(m) \delta_x \delta_y |\gamma_m|^2} \exp(-j\psi_m), \quad (1)$$

where G_m is the antenna gain of element m, and ψ_m is the corresponding phase shift. Variable γ_m is the power ratio of the departure signal to the arrival signal. It can either be a function of s_m or a constant, which is related to the schematic structure of the IOS element. $K^A(m)$ and $K^D(m)$ are the normalized power radiation pattern of the arrival signal and departure signal, respectively.[1] An example of the normalized power radiation pattern is given as following:

$$K^A(m) = |\cos^3 \theta^A(m)|, \quad (2)$$

$$K^D(m) = \begin{cases} |\cos^3 \theta^D(m)|, \tilde{}\theta^D(m) \in (0, \pi/2), \\ \epsilon |\cos^3 (\pi - \theta^D(m))|, \tilde{}\theta^D(m) \in (\pi/2, \pi), \end{cases} \quad (3)$$

where ϵ is a constant parameter that describes the power ratio of the transmissive signal to the reflective signal.[2]

[1]The departure signal can be either transmissive signal or reflective signal.

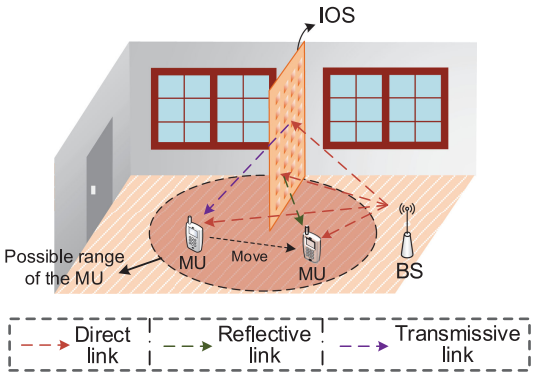

Fig. 3. System model for the IOS-aided downlink cellular system.

III. System Model and Problem Formulation

In this section, we first describe an IOS assisted single MU downlink system, and then introduce the channel model and SE of the IOS-assisted system. Finally, we formulate a downlink SE maximization problem by optimizing the IOS phase shift.

A. Scenario Description

As shown in Fig. 3, we consider a downlink transmission scenario in an indoor environment, which consists of one BS and one MU. We assume that the MU is randomly located in a range denoted by $\mathcal{L}$. Due to the severe channel fading and complicated scattering in the indoor environment, the MU may suffer low quality of service of the communication link to the BS. To tackle this problem, we deploy an IOS in the indoor environment. The power of the received signals at the MU can be improved with either the transmissive signal or the reflective signal of the IOS, and the type of the received signal from the IOS is determined by the current location of the MU. The IOS can be viewed as an antenna array far away from the BS, inherently capable of realizing beamforming via the IOS phase shift design, which will be introduced in detail in Section III-C.

B. Channel Model

The channel from the BS to the MU consists of two parts: the direct path from the BS to the MU bypassing the IOS, and the reflective-transmissive channel that goes through the IOS. The detailed descriptions of the direct path and the reflective-transmissive channel are given in the following.

1) Direct Path Bypassing the IOS: The channel model of the direct path from the BS to the MU is similar to the one in conventional cellular networks, which can be formulated as a Rician channel. The

[2]The value of ϵ is determined by the material of the IOS element [8] which needs to be performed before the IOS deployment. Therefore, the distribution of the MU should be estimated before the IOS deployment.

channel of the direct path from the BS to the MU can be written by

$$h_D = \sqrt{\frac{\kappa}{1+\kappa}} h_D^{\mathrm{LoS}} + \sqrt{\frac{1}{1+\kappa}} h_D^{NLoS}, \tag{4}$$

where κ is the Rician factor indicating the ratio of the LoS component to the non-line-of-sight (NLoS) one, and h_D^{LoS} and h_D^{NLoS} are the LoS and NLoS components of the direct path, respectively. According to [9], the LoS component of the normal channel between the BS and the MU can be given as $h_D^{\mathrm{LoS}} = \sqrt{G^{tx} G^{rx} d_{BS,MU}^{-\alpha}} \exp\left(-j\frac{2\pi}{\lambda} d_{BS,MU}\right)$, where G^{tx} is the transmission antenna gain of the BS antenna, G^{rx} is the receiving antenna gain of the MU, $d_{BS,MU}$ is the distance from the BS to the MU, and α is the path-loss parameter. Similarly, the NLoS component can be written as $h_D^{NLoS} = PL(d_{BS,MU}) h^{SS}$, where $PL(\cdot)$ is the channel gain for the NLoS component, and $h^{SS} \sim \mathcal{CN}(0,1)$ denotes the small-scale NLoS components.

2) Transmissive-Reflective Channel via the IOS: As introduced in Section II, the departure signal of the IOS contains two parts: transmissive signal and reflective signal. The location of the MU determines whether it receives the transmissive signal or the reflective signal. The channel from the BS to the MU via the IOS can be considered as the sum of M channels from the BS to the MU via every IOS element. Since the BS-IOS-MU link is much stronger than the NLoS ones, the channel from the BS to the MU via each IOS element can be modeled as a Racian channel. The channel gain from the BS to the MU via IOS element m is given as

$$h_m = \sqrt{\frac{\kappa}{1+\kappa}} h_m^{\mathrm{LoS}} + \sqrt{\frac{1}{1+\kappa}} h_m^{NLoS}. \tag{5}$$

The LoS component of h_m can be expressed as

$$h_m^{\mathrm{LoS}} = \frac{\lambda \sqrt{G^{tx} F_m^{tx} G^{rx} F^{rx}} \exp\left(\frac{-j2\pi(d_{BS,m}+d_{m,MU})}{\lambda}\right)}{(4\pi)^{\frac{3}{2}} d_{BS,m} d_{m,MU}} \times g_m(\xi^A(m), \xi^D(m), s_m), \tag{6}$$

where λ is the wave length corresponding to the carrier frequency, G^{tx} and G^{rx} are antenna gains of the BS and the MU, respectively, F_m^{tx} is the normalized power gain of the BS antenna in the direction of the m-th IOS element, F_m^{rx} is the normalized power gain of the MU in the direction of IOS element m, $d_{BS,m}$ and $d_{m,MU}$ are the distances from the IOS element m to the BS and to the MU, respectively. $g_m(\xi_k^A(m), \xi^D(m), s_m)$ is the power gain of the signal toward the MU via IOS element m, which is given in (1). The NLoS component of h_m can be written as

$$h_m^{NLoS} = PL(d_{BS,m}) PL(d_{m,MU}) h^{SS}, \tag{7}$$

where $PL(\cdot)$ is the channel gain for the NLoS component, and $h^{SS} \sim \mathcal{CN}(0,1)$ denotes the small-scale NLoS component.

In summary, the channel gain from the BS to the MU can be written as

$$h = \sum_{m=1}^{M} h_m + h_D, \tag{8}$$

where the first term represents the superposition of the transmissive-reflective channel of the M IOS elements, and the second term is the direct path.

C. Spectral Efficiency With IOS Phase Shift Design

In this part, we introduce the IOS phase shift design, with which the power of the signal received by the MU can be improved significantly. According to (8), the received signal at the MU can be expressed as

$$z = \sum_{m=1}^{M} h_m x + h_D x + n, \tag{9}$$

where n is the additive white Gaussian noise (AWGN) at the MU with zero mean and σ^2 as the variance, and x denotes the transmitted signal with $|x|^2 = 1$.

The downlink SE of the MU can be defined as the data rate in bits per second per Hz, which is given as

$$R = \log_2\left(1 + \frac{P|h|^2}{\sigma^2}\right), \tag{10}$$

where P is the transmission power of the BS, which is given as a constant in this paper.

D. Problem Formulation

In this part, we formulate an IOS phase shift design problem to maximize the average downlink SE of the system. As shown in (6) and (10), the SE of the MU is determined by its location and the phase shift of the IOS $\boldsymbol{s}$. Given the MU location $\boldsymbol{l}$, the signal-to-noise ratio at the MUs can be added instructively with proper IOS phase shift design, and the SE can be improved. In the following, we aim to maximize the SE of the MU randomly distributed in the range of $\mathcal{L}$ by optimizing the phase shift of IOS $\boldsymbol{s}$, and then the problem can be formulated as

$$\max_{\boldsymbol{s}} \ R, \forall\, \boldsymbol{l} \in \mathcal{L}, \tag{11a}$$

$$\text{s.t. } s_m \in \mathcal{S}_a, m = 1, 2, \cdots M. \tag{11b}$$

Constraint (11b) is the feasible set for the phase shifts of each IOS element.

IV. IOS Phase Shift Design

In this section, we first relax the variable in problem (11) and discuss the SE maximization problem with continuous IOS phase shifts, and then propose a branch-and-bound based algorithm to design the IOS phase shift in finite set $\mathcal{S}_a$.

A. Continuous IOS Phase Shift Design

As shown in (4), the channel of the direct path is not affected by the phase shift of the IOS, and thus we only need to optimize the SE of the BS-IOS-MU link. Moreover, the BS-IOS-MU link is modeled as a Racian channel given in (5), whose NLoS component is not affected by the phase shift of the IOS. Therefore, problem (11) can be simplified as maximizing the SE of the LoS component of the BS-IOS-MU link, which is shown as

$$\max_{\boldsymbol{s}} \ \log_2\left(1 + \frac{P|\sum_{m=1}^{M} h_m^{\mathrm{LoS}} + h_D|^2}{\sigma^2}\right), \forall\, \boldsymbol{l} \in \mathcal{L}, \tag{12a}$$

$$\text{s.t. } s_m \in \mathcal{S}_a, m = 1, 2, \cdots M. \tag{12b}$$

Problem (12) is an integer optimization problem, which cannot be solved by the optimization methods for continuous variables. In the following, we first solve the problem with $\boldsymbol{s}$ being relaxed to a continuous variable, and then we propose a branch-and-bound based algorithm to design the discrete phase shift for each IOS element.

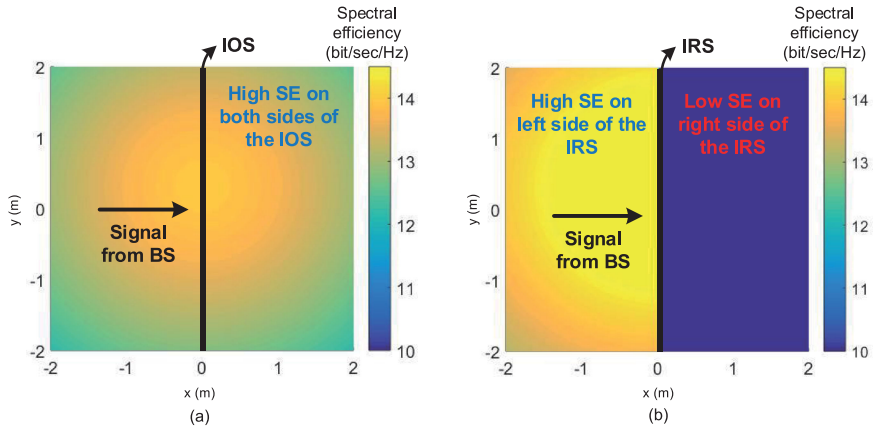

Fig. 4. Simulation for maximum SE. (a) IOS system. (b) IRS system.

Proposition 1: When the power ratio of the departure signal to the arrival signal γ_m is considered as a constant, the optimal phase shift of each element satisfies

$$\psi_m = \frac{2\pi}{\lambda}(d_{BS,MU} - d_{BS,m} - d_{m,MU}), m = 1, \ldots, M. \quad (13)$$

Proof: See Appendix A. ■

B. Finite IOS Phase Shift Design

The optimal solution proposed in Proposition 1 cannot be obtained by the IOS elements with a finite set of phase shift $\mathcal{S}_a$. For IOS element m, we denote its optimal phase shift by ψ_m^{opt}. For IOS element m, its phase solution to problem (11) is one of the two consecutive phase shifts of s_m and s_{m+1}, which satisfies $\psi_m \leq \psi_m^{\text{opt}} \leq \psi_{m+1}$. In the following, we propose a branch-and-bound based algorithm to solve the IOS phase shift design in the finite set $\mathcal{S}_a$ efficiently.

The solution space of IOS phase shift $\boldsymbol{s}$ can be considered as a binary tree structure. Each node of the tree contains the phase shift of all the IOS elements, i.e., $\boldsymbol{s} = (s_1, \ldots, s_M)$. At the root node, all the variables in $\boldsymbol{s}$ are unfixed. The value of an unfixed variable at a father node can be either s_m or s_{m+1}, which branches the node into two child nodes. The objective of the proposed algorithm is to search the tree for the optimal solution of problem (11) with the following three steps.

Step 1. Initialization: We first set a random IOS phase shift, and the corresponding SE is given as the lower bound of the solution.

Step 2. Bound Calculation: We then start to search the optimal solution from the root node. On each node we first evaluate the upper bound of the objective function with variable relaxation, and the upper bound can be calculated with the phase shift solution proposed in Proposition 1.

Step 3. Variable Fixation: In this step, we prune the branches whose upper bounds are below the value of the current solution. When a solution that outperforms the current solution is found, we replace the current solution with the new one, and continue the branch-and-bound algorithm. The phase shifts of an element is fixed when only one feasible value satisfies the bound requirements.

The algorithm terminates when all the element phase shifts are fixed, and the corresponding current solution is the final solution of problem (11). The proposed algorithm that solves problem (11) is summarized as Algorithm 1.

Algorithm 1: IOS Phase Shift Design Algorithm.

Initialization: Compute an initial solution $\boldsymbol{s}$ to problem (12) and set the SE as the lower bound R_{lb}
While Not all nodes are visited or pruned
  Calculate the upper bound of the current node R_{ub}
  If $R_{ub} < R_{lb}$: Prune this branch
  If Variable s_m is fixed: Go to the node with s_m
  Else Generate two new nodes by setting an unfixed variable at s_m and s_{m+1}
    Go to a node that has not been visited or pruned
  If The current node has a corresponding SE R_{curr}:
    If $R_{curr} > R_{lb}$: $R_{lb} = R_{curr}$
Output: $\boldsymbol{s}$;

V. Simulation Results

In this section, we evaluate the performance of the IOS assisted system with the proposed algorithm in an indoor environment, and compare it with the IRS assisted system as proposed in [12], [13] and the conventional cellular system. In the IRS assisted system, the IRS only reflects the signals from the BS to the MU, and no transmissive signal is considered. In the conventional cellular system, we only consider the direct link from the BS to the MU. In our simulation, we set the height of the BS and the center of the IOS as 2 m, and the distance between the BS and the IOS being 500 m. The MU is randomly deployed within a circle of radius 2 m centering at the IRS, and the results present below are the average performance of over 10000 instances of the Monte Carlo simulation. The maximum transmit power of the BS P_B is 40 dBm, the power of the AWGN is -96 dBm, and the IOS element separation is 0.03 m. The power ratio of the transmissive signal to the reflective signal ϵ is set as 1, the number of phase shifts for each IOS element is set as $S_a = 4$.

Fig. 4 shows the maximum SE of the MU on different locations, with the BS on the left side of the surface. An IOS/IRS with the length of 4 m and the height of 0.6 m is deployed at the line segment ((0, -2), (0, 2)), and the BS is deployed at (-500, 0). In the IOS system, the SE on either side of the surface can be improved. A higher SE can be obtained when the MU is closer to the center of the IOS, where the reflective-transmissive channel has a better quality. In the IRS system, the MU has a high SE only when it is on the left side of the surface.

Fig. 5 depicts the relation between the average SE of the MU and the size of the IOS. The average SE is defined as the expectation of SE R with the random distribution of the MU. The IOS is considered as a square array with $\sqrt{M}$ elements on each line and each row. The SE increases with the number of IOS elements, and the growth rate gradually slows down with the IOS size. An IOS with 10×10 elements improves the average SE for about 20 times when compared

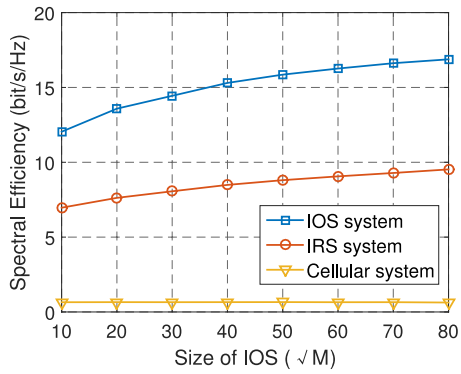

Fig. 5. Size of IOS vs. SE.

to the conventional cellular system, while an IRS of the same size only improves the average SE for about 12 times. The performance difference between the two systems is caused by the service coverage. The IOS can improve the average SE of the MU on either side of the surface, while the IRS can only improve that of the MU on one side.

VI. Conclusion

In this paper, we have studied an IOS-assisted downlink system. The IOS is capable to enhance the received signal of the MU on either side of it with IOS phase shift design. We have formulated an IOS phase shift design problem to maximize the SE of the system. The optimal phase shifts of the IOS elements have been solved, and an algorithm that designs the IOS phase shift in the finite set has been proposed. Simulation results have shown that the IOS significantly extends the service coverage of the BS when compared to the IRS. An IOS with a larger size can provide a higher SE for the MU, while the growth rate reduces with more IOS elements.

Appendix A
Proof of Proposition 1

Given the location of the BS, IOS, and MU, the SE maximization problem can be simplified as maximizing the channel gain, and the relaxed problem can be expressed as

$$\max_{\boldsymbol{s}} \ \mathbb{E}\left(|h|^2\right),$$
$$\text{s.t. } 0 \le \psi_m < 2\pi, m = 1, 2, \cdots M. \tag{14}$$

We then substitute (4) and (5) into (8). Given that h_m^{NLoS} is zero mean and is independent for different elements, (14) can be converted to $\mathbb{E}(|h|^2) = \sum_{m=1}^{M}(\frac{\kappa}{1+\kappa}A\exp(\frac{-j2\pi(d_{BS,m}+d_{m,MU})}{\lambda})\exp(-j\psi_m) + \frac{1}{1+\kappa}PL(d_{BS,m})PL(d_{m,MU})) + \frac{\kappa}{1+\kappa}PL^{\text{LoS}}\exp(\frac{-j2\pi(d_{BS,MU})}{\lambda}) + \frac{1}{1+\kappa}PL(d_{BS,MU})$, where $A = \frac{\lambda\sqrt{G^{tx}F_m^{tx}G^{rx}F^{rx}}\times\sqrt{G_m K^A(m)K^D(m)\delta_x\delta_y|\gamma_m|^2}}{(4\pi)^{\frac{3}{2}}d_{BS,m}d_{m,MU}}$ is not affected by the phase shift of the IOS. PL^{LoS} is the LoS pathloss of the direct link, and $PL(d_{BS,MU})$ is the NLoS pathloss of the direct link, which are also not affected by the phase shift of the IOS. To maximize (14), the phase shift term of each element $\exp(\frac{-j(2\pi(d_{BS,m}+d_{m,MU})+\psi_m)}{\lambda})$ should be consistent with the direct path, i.e., $\psi_m + \frac{2\pi(d_{BS,m}+d_{m,MU})}{\lambda} = \frac{2\pi(d_{BS,MU})}{\lambda}$. Therefore, the optimal solution of element m satisfies

$$\psi_m = \frac{2\pi}{\lambda}(d_{BS,MU} - d_{BS,m} - d_{m,MU}). \tag{15}$$

References

[1] M. Renzo *et al.*, "Smart radio environments empowered by reconfigurable ai meta-surfaces: An idea whose time has come," *EURASIP J. Wireless Commun. Netw.*, vol. 2019, no. 129, pp. 1–20, May 2019.
[2] M. A. Elmossallamy, H. Zhang, L. Song, K. Seddik, Z. Han, and G. Y. Li, "Reconfigurable intelligent surfaces for wireless communications: Principles, challenges, and opportunities," *IEEE Trans. Cogn. Commun. Netw.*, vol. 6, no. 3, pp. 990–1002, Sep. 2020.
[3] J. Hu *et al.*, "Reconfigurable intelligent surfaces based radio-frequency sensing: Design, optimization, and implementation," *IEEE J. Sel. Areas Commun.*, to be published.
[4] C. Huang, A. Zappone, G. C. Alexandropoulos, M. Debbah, and C. Yuen, "Reconfigurable intelligent surfaces for energy efficiency in wireless communication," *IEEE Trans. Wireless Commun.*, vol. 18, no. 8, pp. 4157–4170, Aug. 2019.
[5] H. Zhang, B. Di, L. Song, and Z. Han, "Reconfigurable intelligent surfaces assisted communications with limited phase shifts: How many phase shifts are enough?," *IEEE Trans. Veh. Technol.*, vol. 69, no. 4, pp. 4498–4502, Apr. 2020.
[6] V. Arun and H. Balakrishnan, "RFocus: Practical beamforming for small devices," Accessed: May 2019. [Online]. Available: https://arxiv.org/abs/1905.05130
[7] W. Tang *et al.*, "Wireless communications with reconfigurable intelligent surface: Path loss modeling and experimental measurement," Accessed: Nov. 2019. [Online]. Available: https://arxiv.org/abs/1911.05326
[8] C. Pfeiffer and A. Grbic, "Metamaterial Huygens' surfaces: Tailoring wave fronts with reflectionless sheets," *Phys. Rev. Lett.*, vol. 110, no. 197401, pp. 1–5, May 2013.
[9] A. Goldsmith, *Wireless Communications*. Cambridge, U.K.: Cambridge Press, 2005.
[10] B. Di, H. Zhang, L. Song, Y. Li, Z. Han, and H. V. Poor, "Hybrid beamforming for reconfigurable intelligent surface based multi-user communications: Achievable rates with limited discrete phase shifts," *IEEE J. Sel. Areas Commun.*, vol. 38, no. 8, pp. 1809–1822, Aug. 2020.
[11] D. Tse and P. Viswanath, *Fundamentals of Wireless Communications*. Cambridge, U.K.: Cambridge Univ. Press, 2005.
[12] S. Abeywickrama, R. Zhang, and C. Yuen, "Intelligent reflecting surface: Practical phase shift model and beamforming optimization," *IEEE Trans. Commun.*, vol. 68, no. 9, pp. 5849–5863, Sep. 2020.
[13] B. Di, H. Zhang, L. Li, L. Song, Y. Li, and Z. Han, "Practical hybrid beamforming with finite-resolution phase shifters for reconfigurable intelligent surface based multi-user communications," *IEEE Trans. Veh. Technol.*, vol. 69, no. 4, pp. 4565–4570, Apr. 2020.